Soot in a Time-Varying Flame: Are Scattering and Extinction Measurements Sufficient ?

Joel E. Harrington, Christopher R. Shaddix and Kermit C. Smyth
Fire Science Division
National Institute of Standards and Technology
Gaithersburg, Md 20899

Summary

Laser-sheet scattering images of the soot region in a time-varying methane/air diffusion flame, whose fuel flow is modulated at a frequency matching the 10.13 Hz laser repetition rate, show at least a factor of ten enhancement in volume integrated scattering intensity when compared with images of a steady-state flame with the same mean fuel and air co-flows (Figure 4). However, only a small enhancement (~50%) appears in a comparison between the peak values of what is commonly interpreted as soot volume fraction, obtained through tomographic reconstruction of HeNe and Ar ion extinction measurements (Figure 6). The time-averaged soot volume fraction in the entire flame is identical, within our measurement error, for the steady and time-varying flames. We anticipate an explanation of our scattering and extinction results based on changes in particle size and morphology induced by a different time-temperature history in the flickering flame.

Introduction

Soot formation is especially sensitive to local combustion conditions since pre-particle inception chemistry is relatively slow [1]. In co-flowing, steady-state laminar diffusion flames, the earliest soot particles form near the high-temperature, primary reaction zone and then move to richer and cooler regions through convection and thermophoresis [2]. As a consequence, soot inception, mass growth and oxidation occur sequentially [3]. Because unsteady flames (naturally flickering, forced or turbulent) provide residence times, temperature histories, local stoichiometries, strain and scalar dissipation rates unavailable in corresponding steady flames, characteristics of the soot field might be expected to change as well.

The natural flame flicker frequency, f, in axisymmetric diffusion flames correlates with the fuel tube diameter, D, as $f \approx 1.5/ D^{1/2}$, where D has units of meters [4,5]. Common laboratory burners produce flickering flames with frequencies between 10 and 20 Hz. In these flames, buoyancy induces flickering through large outer vortex production at the interface between the hot combusting gases and the cooler co-flow: this process has been described as a modified Kelvin-Helmholtz hydrodynamic instability [6]. To create a reproducible environment for examining vortices and their interaction with the flame, an acoustic perturbation can be applied to the fuel stream [7] at a frequency close to the natural flicker frequency. Images obtained from forced flames are qualitatively similar to those from naturally flickering flames so we presume that the underlying physics and chemistry are also similar.

In this study we compare soot extinction and scattering results from a steady-state methane/air flame with extinction and scattering from a forced unsteady flame with the same mean fuel flow and air co-flow rates.

Experiment

The burner and scattering experiment have been described in detail previously [8]. Figure 1 shows a schematic of the scattering experiment.

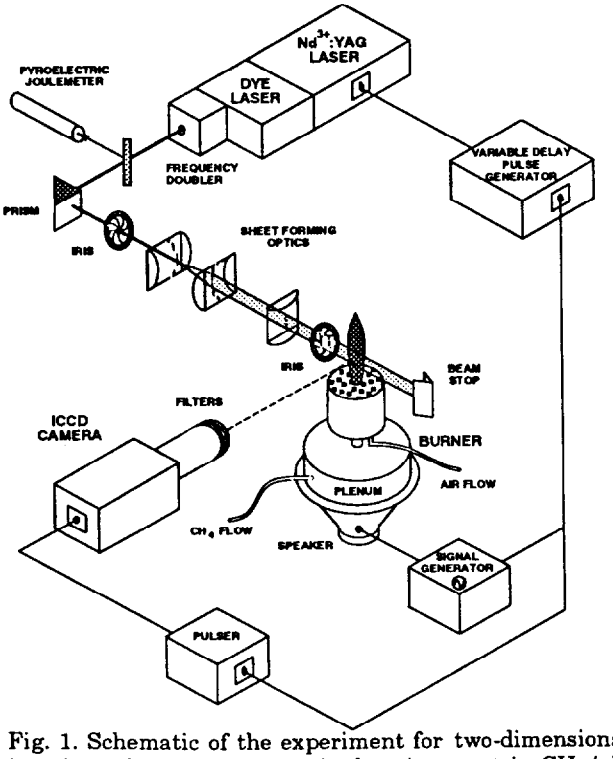

Fig. 1. Schematic of the experiment for two-dimensional imaging of acoustically excited, axisymmetric CH_4/air diffusion flames. The flame is phase-locked to the pulsed dye laser system operating at 10.13 Hz.

Combustion Institute/Eastern States Section. Chemical and Physical Processes in Combustion. Technical Meeting, 1993. October 25-27, 1993, Princeton, NJ, 390-393 pp, 1993.

A coannular axisymmetric burner with a 1.1 cm diameter fuel tube surrounded by a 10.2 cm air annulus supports an unconfined laminar flame. The mean methane cold flow velocity and air co-flow were 7.9 cm/s for both the steady and forced flames. A loudspeaker attached to the burner plenum locks the frequency of the pulsing flame to the 10.13 Hz repetition rate of the dye laser system. Both the phase and the amplitude of the imposed sign wave are variable; all data presented here were taken with 0.75 V peak-to-peak sine wave forcing.

Nd^{3+}:YAG pumped dye laser light at 567 nm is frequency doubled to 283.55 nm for imaging OH fluorescence and soot scattering or 283.50 nm for soot scattering alone. Cylindrical lenses form the frequency doubled light into a vertical sheet. A Babinet-Soleil compensator controls the polarization of the input beam relative to the detection axis. A UV intensified CCD camera collects the scattered light and fluorescence at 90 to the laser propagation axis. To attenuate the scattered light to a level comparable to the OH fluorescence, glass filters are placed in front of the camera lens.

Images shown are from single laser shots. The 576 x 384 array of pixels is binned 3 x 3 into a 192 x 128 array to reduce the effects of shot noise. Each image is corrected by subtracting a background taken before each set images, dividing by the flat field response of the pixels as measured by illumination with a standard tungsten lamp, and dividing by the instantaneous laser sheet intensity. The beam intensity and its spatial distribution are determined by imaging the laser sheet directly onto the camera for each shot. A translation stage sets the burner height so that each set of four or five consecutive images can be stacked to show the full two-dimensional extent of the flame. Several of the stacked images shown have been shifted slightly right or left to compensate for minor flame wobble.

Tomographic inversion of line-of-sight extinction at both HeNe (632.8 nm) and Ar ion (454.5 nm) wavelengths determines the distribution of soot volume fraction in the flames, neglecting contributions to the extinction from scattering and molecular absorption. Figure 2 shows a schematic of the extinction apparatus. A power stabilizer reduces the noise in the input laser beams to the order of 0.1%, allowing measurement of extinction on the order of 0.01% after averaging. For extinction measurements in these weakly sooting flames both laser power stability and minimization of beam movement (from thermal lensing) on the photodiode [9] are critical. A digital oscilloscope collects and averages 200 time records of the laser extinction at a single height and radial position. For each height, data are collected every 0.25 mm over the width of the flame. In the steady flame, full radial sets of data are taken every 10 mm in height starting 20 mm above the burner lip; in the forced flame data are taken every 20 mm.

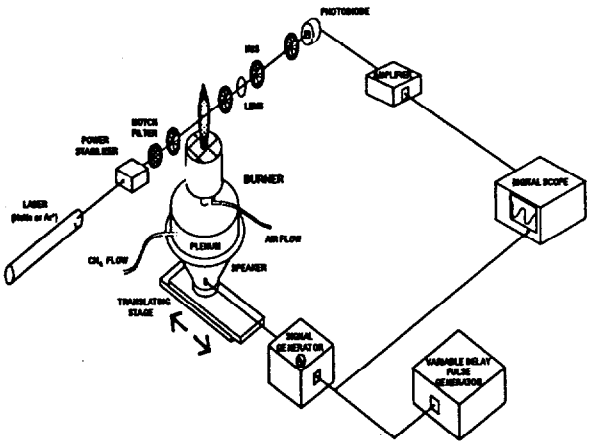

Fig 2. Schematic of the experiment for measurement of extinction along chords of the axisymmetric steady and time-varying flames.

Results

Images of scattering and OH fluorescence at ten different phases of a single flame flicker cycle are shown in Figure 3. The relative time of each image is expressed as a percentage of the full 99 ms period of flame flickering. Zero phase is arbitrary. No soot breaks out of these methane flames under any of our experimental conditions; the OH fluorescence marks a continuous high-temperature reaction zone completely enclosing and eventually burning through the soot layer.

The time-averaged, volume integrated soot scattering signal is greater in the time-varying flame by at least a factor 10 over the steady flame (Figure 4). Instantaneous point scattering is as much as 15 times higher in the flickering flame. The peaked structure in the time-averaged soot scattering for the flickering flame in Figure 4 is most likely a result of having only ten scattering measurements per phase cycle. Averaging more points in the flickering cycle would produce a smoother curve, but the volume integrated result would not change significantly.

Three-point Abel inversion [10] of the extinction data produces radial reconstructions of the soot field for each point in phase and height above the burner. The soot volume fraction, f_V, can be calculated with $f_V = \lambda\, k_{ext}/6\, E(\tilde{n})$ [11], where λ is wavelength of the laser light, k_{ext} is the

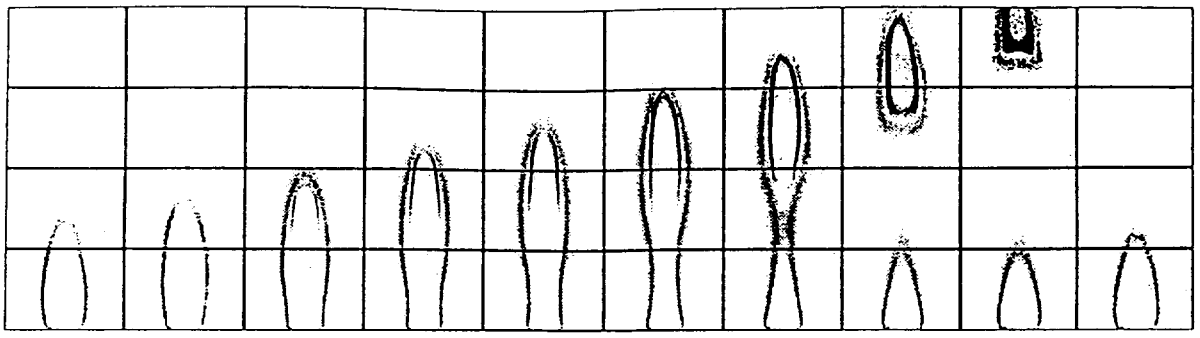

Fig. 3. Soot scattering and OH laser-induced fluorescence in a time-varying laminar CH_4/air diffusion flame using horizontally polarized light at 283.55 nm. Inner intense signals are from soot scattering; more diffuse outline is OH fluorescence. Ten phases (arbitrary zero) are shown corresponding to time intervals of 9.9 ms. The excitation voltage was 0.75 V. At each phase four separate single-shot images are stacked to show most of the area of the flame.

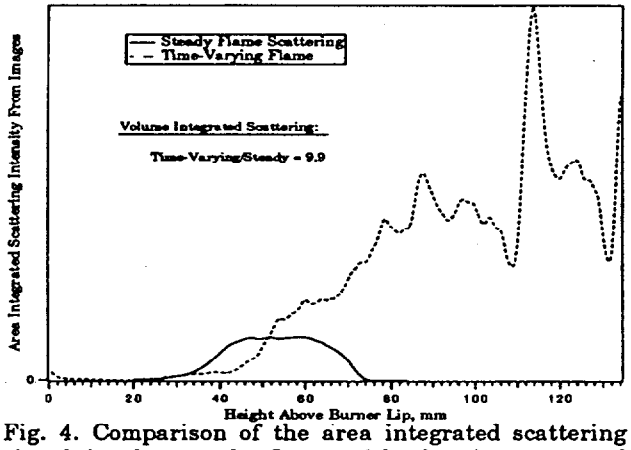

Fig. 4. Comparison of the area integrated scattering signal in the steady flame with the time-averaged scattering in the flickering flame as a function of height above the burner lip.

extinction coefficient calculated by the Abel inversion, $E(\tilde{n}) = -Im[(\tilde{n}^2-1)/(\tilde{n}^2+2)]$ and $\tilde{n}$ is the complex index of refraction. We use $\tilde{n}$ = 1.57 - 0.56i [11] in order to make direct comparisons with the results of Santoro [11,12].

Reconstructed radial profiles of soot volume fraction for the steady methane/air flame are in good agreement with data from Richardson and Santoro [12]. Results from the flickering flame are shown in Figure 5. Eighty instantaneous radial profiles of soot volume fraction are offset in 1 ms steps for each height above the burner lip. The plots show from 20 to 99% of full phase corresponding to the scattering phases shown in Figure 3. Peak soot volume fraction in the time-varying flame is at most a factor of two higher than in the steady flame. However, the time-averaged, volume integrated soot in the two flames is identical (3.3×10^{-4} mm^3); see Figure 6.

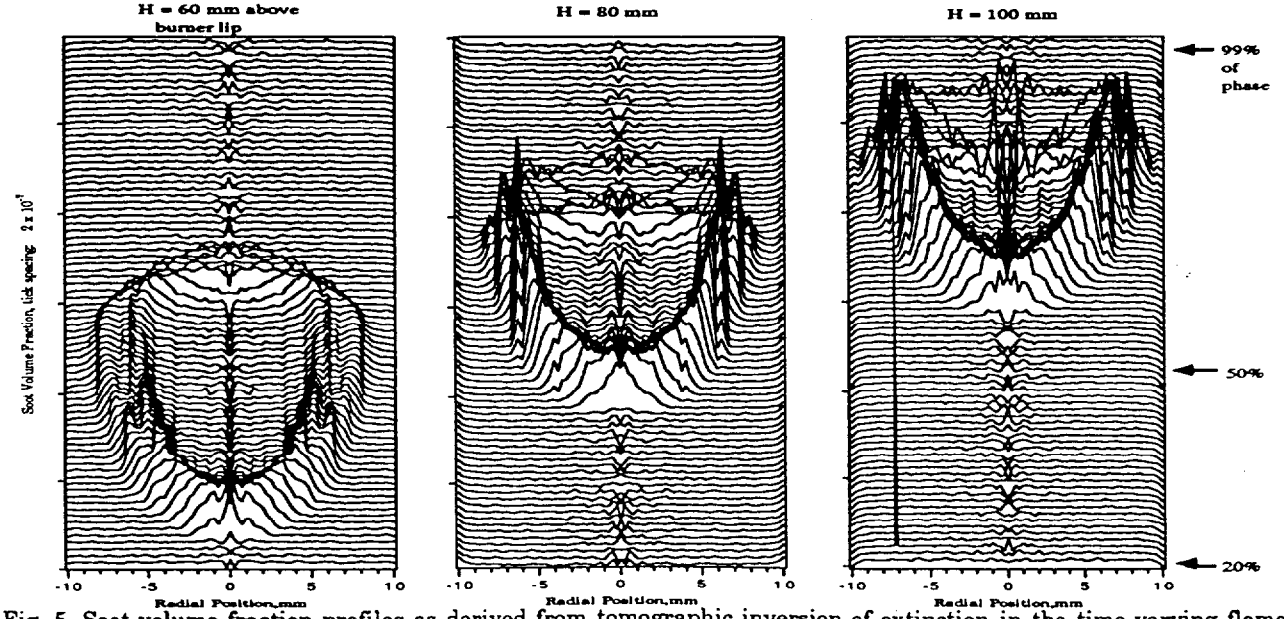

Fig. 5. Soot volume fraction profiles as derived from tomographic inversion of extinction in the time-varying flame, offset in equal time steps (or percentage of full phase time) at three heights above the burner lip. Eighty profiles in each plot correspond to 80 ms of the 99 ms period. Earliest soot profiles correspond to the top of the flame.

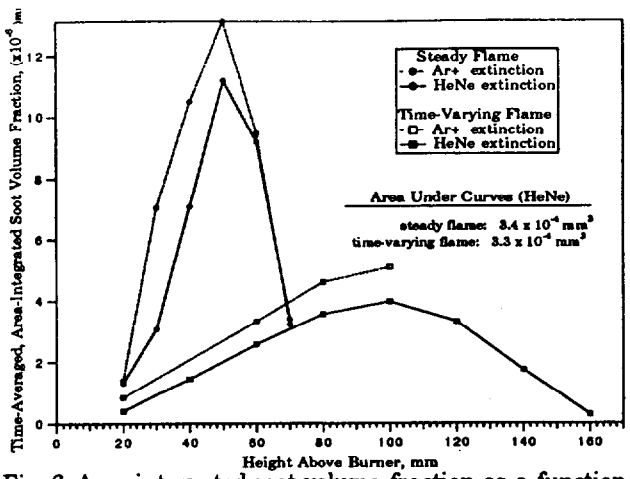

Fig. 6. Area integrated soot volume fraction as a function of height above the burner lip for two wavelengths in the steady and time-varying flames. The time-averaged, volume integrated soot volume fraction is identical within our error for the steady and time-varying flames.

Low in the flame, radial profiles of the 454.5 nm Ar ion reconstructions exhibit stronger extinction extending closer to the centerline than the 632.8 nm HeNe data. Higher in the steady flame, radial profiles from both wavelength extinction measurements agree. Differences in the profiles at the two wavelengths are likely due to extinction from molecular species and microparticles. Extinction is probably dominated by polynuclear aromatic hydrocarbons that absorb more strongly at shorter wavelengths [13]; we are pursuing experiments which compare molecular fluorescence in the steady and time-varying flames.

Discussion

Soot scattering signals increase strongly when a sinusoidal perturbation is applied to the fuel flow of a steady methane flame, causing it to clip off and flicker. However, the maximum local soot volume fraction increases by only about 50%, and the time-averaged, volume-integrated soot volume fraction is unchanged. Rayleigh-Mie theory predicts that the local ratio of the scattering to extinction signals is proportional to the cube of the particle diameter [11]. This ratio increases by a factor of six to ten relative to steady values in the upper regions of the flickering flame, suggesting that mean particle diameters have roughly doubled. For a monodisperse distribution of spherical particles that are much smaller than the wavelength of the incident radiation, the same experimental results predict a factor of five decrease in the local particle number density. This description neglects any possible effects of non-spherical soot geometries (e.g., chains of primary particles), which are known to form through agglomeration in similar diffusion flames [3]. Experiments are underway to more thoroughly investigate the soot size and morphology and independently check the soot volume fraction measurements using laser-induced incandescence [14,15].

References

1. Glassman, I., *Twenty-Second Symposium (International) on Combustion,* The Combustion Institute, Pittsburgh, 1988, p. 295 and references therein.

2. Santoro, R.J., Yeh, T.T., Horvath, J.J., and Semerjian, H.G., *Combustion Science and Technology* **53**, 89 (1987).

3. Dobbins, R.A., Santoro, R.J., and Semerjian, H.G., *Twenty-Third Symposium (International) on Combustion,* The Combustion Institute, Pittsburgh, 1990, p. 1525.

4. Hamins, A., Yang, J.C., and Kashiwagi, T., *Twenty-Fourth Symposium (International) on Combustion,* The Combustion Institute, Pittsburgh, 1992, p. 1695 and references therein.

5. Cetegen, B.M., and Ahmed, T.A., *Combustion and Flame* 93, 157 (1993).

6. Buckmaster, J., and Peters, N., *Twenty-First Symposium (International) on Combustion,* The Combustion Institute, Pittsburgh, 1986, p. 1829.

7. See, for example, G.S. Lewis, B.J. Cantwell, U. Vandsberger, G.S., and Bowman, C.T., *Twenty-Second Symposium (International) on Combustion,* The Combustion Institute, Pittsburgh, 1988 p. 515.

8. Smyth, K.C., Harrington, J.E., Johnsson, E.L. and Pitts, W.M., *Combustion and Flame,* in press.

9. Minimization of a similar beam-steering problem in flame holography is described in Montgomery, G.P. and Reuss, D.L. *Applied Optics* 21, 1373 (1982).

10. Dasch, C.J., *Applied Optics* 31, p. 1146 (1992).
Thanks to J. Houston Miller for providing a Pascal program for the 3-point Abel inversion.

11. Santoro, R.J., Semerjian, H.G., and Dobbins, R.A., *Combustion and Flame* 51, 203 (1983).

12. Richardson, T.F., and Santoro, R.J., private communication.

13. Miller, J.H., Mallard, W.G., and Smyth, K.C., *Combustion and Flame* 47, 205 (1982).

14. Melton, L.A., *Applied Optics* 23, 2201 (1984).

15. Tait, N.P., and Greenhalgh, D.A., *Proceedings of the "Optical Methods and Data Processing in Heat Transfer and Fluid Flow" Conference*, London, April 1992.